

UC Davis

UC Davis Previously Published Works

Title

Tumoral Densities of T-Cells and Mast Cells Are Associated With Recurrence in Early-Stage Lung Adenocarcinoma.

Permalink

<https://escholarship.org/uc/item/0xc778nw>

Journal

JTO Clinical and Research Reports, 4(9)

Authors

Kammer, Michael

Rowe, Dianna

Chen, Sheau-Chiann

et al.

Publication Date

2023-09-01

DOI

10.1016/j.jtocrr.2023.100504

Copyright Information

This work is made available under the terms of a Creative Commons Attribution-NonCommercial-NoDerivatives License, available at

<https://creativecommons.org/licenses/by-nc-nd/4.0/>

Peer reviewed

Tumoral Densities of T-Cells and Mast Cells Are Associated With Recurrence in Early-Stage Lung Adenocarcinoma



Michael N. Kammer, PhD,^{a,b,*} Hidetoshi Mori, PhD,^c Dianna J. Rowe, BS,^a Sheau-Chiann Chen, PhD,^d Georgii Vasiukov, PhD,^a Thomas Atwater, MD,^a Maria Fernanda Senosain, PhD,^a Sanja Antic, MD,^a Yong Zou, MS,^a Heidi Chen, PhD,^d Tobias Peikert, MD,^e Steve Deppen, PhD,^{f,g} Eric L. Grogan, MD,^{f,g} Pierre P. Massion, MD,^{a,b} Steve Dubinett, MD,^h Marc Lenburg, PhD,ⁱ Alexander Borowsky, MD,^c Fabien Maldonado, MD^a

^aDivision of Allergy, Pulmonary, and Critical Care Medicine, Vanderbilt University Medical Center, Nashville, Tennessee

^bVanderbilt Ingram Cancer Center, Vanderbilt University Medical Center, Nashville, Tennessee

^cDepartment of Pathology, University of California, Davis, Davis, California

^dDepartment of Biostatistics, Vanderbilt University Medical Center, Nashville, Tennessee

^eDepartment of Pulmonary and Critical Care Medicine, Mayo Clinic, Rochester, Minnesota

^fDivision of Thoracic Surgery, Vanderbilt University Medical Center, Nashville, Tennessee

^gVA Tennessee Valley Healthcare System, Nashville, Tennessee

^hDavid Geffen School of Medicine at The University of California Los Angeles (UCLA), Los Angeles, California

ⁱSchool of Medicine, Boston University, Boston, Massachusetts

Received 6 September 2022; revised 1 March 2023; accepted 17 March 2023

Available online - 23 March 2023

ABSTRACT

Introduction: Lung cancer is the deadliest cancer in the United States and worldwide, and lung adenocarcinoma (LUAD) is the most prevalent histologic subtype in the United States. LUAD exhibits a wide range of aggressiveness and risk of recurrence, but the biological underpinnings of this behavior are poorly understood. Past studies have focused on the biological characteristics of the tumor itself, but the ability of the immune response to contain tumor growth represents an alternative or complementary hypothesis. Emerging technologies enable us to investigate the spatial distribution of specific cell types within the tumor nest and characterize this immune response. This study aimed to investigate the association between immune cell density within the primary tumor and recurrence-free survival (RFS) in stage I and II LUAD.

Methods: This study is a prospective collection with retrospective evaluation. A total of 100 patients with surgically resected LUAD and at least 5-year follow-ups, including 69 stage I and 31 stages II tumors, were enrolled. Multiplexed immunohistochemistry panels for immune markers were used for measurement.

Results: Cox regression models adjusted for sex and EGFR mutation status revealed that the risk of recurrence was reduced by 50% for the unit of one interquartile range

(IQR) change in the tumoral T-cell (adjusted hazard ratio per IQR increase = 0.50, 95% confidence interval: 0.27–0.93) and decreased by 64% in mast cell density (adjusted hazard ratio per IQR increase = 0.36, confidence interval: 0.15–0.84). The analyses were reported without the type I error correction for the multiple types of immune cell testing.

Conclusions: Analysis of the density of immune cells within the tumor and surrounding stroma reveals an association between the density of T-cells and RFS and between mast cells and RFS in early-stage LUAD. This preliminary result is

*Corresponding author.

Disclosure: The authors declare no conflict of interest.

Address for correspondence: Michael N. Kammer, PhD, Division of Allergy, Pulmonary and Critical Care Medicine, Vanderbilt Ingram Cancer Center, 638 Preston Research Building, 2220 Pierce Ave, Nashville, TN 37235. E-mail: michael.kammer@vumc.org

Cite this article as: Kammer MN, Mori H, Rowe DJ, et al. Tumoral densities of T-Cells and mast cells are associated with recurrence in early-stage lung adenocarcinoma. *JTO Clin Res Rep.* 2023;4:100504.

© 2023 The Authors. Published by Elsevier Inc. on behalf of the International Association for the Study of Lung Cancer. This is an open access article under the CC BY-NC-ND license (<http://creativecommons.org/licenses/by-nc-nd/4.0/>).

ISSN: 2666-3643

<https://doi.org/10.1016/j.jtocrr.2023.100504>

a limited study with a small sample size and a lack of an independent validation set.

© 2023 The Authors. Published by Elsevier Inc. on behalf of the International Association for the Study of Lung Cancer. This is an open access article under the CC BY-NC-ND license (<http://creativecommons.org/licenses/by-nc-nd/4.0/>).

Keywords: T-cells; Mast cells; Adenocarcinoma; Lung cancer; Recurrence

Introduction

Lung cancer is the most prevalent cancer in the United States and the world and kills more people than any other cancer.¹ The landscape of cancer has changed over the past 20 years, and lung adenocarcinoma (LUAD) is now the most common lung cancer subtype in the United States.² LUAD exhibits a broad spectrum of biological behaviors, ranging from highly aggressive to indolent. Aggressive LUADs require prompt management to improve survival, whereas indolent tumors may represent overdiagnosed or overtreated lesions.³ The biological determinants of this broad spectrum of aggressiveness remain unclear, and current management of LUAD remains largely on the basis of tumor stage and mutation status, ignoring the biological variability in aggressiveness.

Past studies of LUAD aggressiveness have almost exclusively focused on molecular or genetic features of the tumor itself.^{4–6} Comparatively, the role of the immune system, and specifically the tumor immune microenvironment (TME) in LUAD has received less attention and studies have yielded conflicting results. For example, it is well documented that immune cell-tumor interactions play an important role in tumor progression, tumor cell proliferation, and tumor death or survival.^{7,8} The prevalence of certain immune cell types and their distribution in the tissue has been associated with outcomes; for example, higher tumor-infiltrating lymphocyte (TIL) density has been found to be associated with increased overall survival in many types of cancer, including NSCLC.^{9,10} Specifically, high densities of intratumoral,^{11–16} CD4+ T-cells,^{17,18} and CD8+ T-cells^{12,15,17,19–22} have been reported in multiple studies to confer a favorable prognosis, whereas high FoxP3+ immune cell and T helper type 2 T-cell density is associated with a worse prognosis.^{10,23} Recently, the characteristics of immune cells were found to be associated with indolent or aggressive behaviors in LUAD.²⁴ Because of their role in immune modulation, investigations of tumor-associated myeloid cells have become a focus of targeted therapeutics research,²⁵ and

mast cell density has been correlated with prognosis in early lung cancer.²⁶

In this study, we aimed to investigate the relationship between immune infiltration in the primary tumor and cancer recurrence after resection and to test the hypothesis that there is an association between the density of myeloid and lymphoid cells within the tumor nest of surgically resected adenocarcinomas and recurrence-free survival (RFS). A better understanding of the interplay between the TME and the likelihood of recurrence could help to understand the determinants of the biological behavior of LUAD. In addition, the use of the TME as a biomarker of risk of recurrence could ultimately guide individualized adjuvant or neoadjuvant treatment and a follow-up approach specifically tailored to each patient. This study uses a novel technology, multiplexed immunohistochemistry (mxIHC) staining, to analyze the spatial relationships between the immune populations and the tumor. We assessed whether there was a difference in RFS that was associated with these immune populations.

Materials and Methods

Tissue samples from prospectively enrolled patients with surgically resected lung primary adenocarcinoma who underwent treatment at Vanderbilt University Medical Center (Nashville, TN) from 2005 to 2015 were used in this study. Tissue collection was approved by Vanderbilt University Medical Center (institutional review board [IRB] protocol 000616), in which informed consent was obtained from the patients before surgical resection. Inclusion criteria were the following: (1) histologic diagnosis-confirmed lung primary local adenocarcinoma with first-line surgery, for which a tumor board adjudicated the patient as free from disease after resection or resection with adjuvant therapy, and the tumor board concluded there was no evidence of metastasis; (2) genetic testing results are available in the patient's medical record (FoundationOne CDx, [Foundation Medicine, Cambridge, MA]); and (3) no evidence of metastasis. All patients with banked tumor tissue consented for research under IRB 000616 that met these criteria were included in the study.

Patients underwent FoundationOne CDx genetic mutation testing according to the standard of care, which looked for mutations in the following genes: EGFR, KRAS, BRAF, PIK3CA, and AKT1. Patient health history was recorded at the time of diagnosis, including age, sex, smoking status, and previous cancer status. Chemotherapy status indicates patients who underwent chemotherapy either before or after their surgical resection, but before the recurrence. Race, smoking status, and age were self-reported. A radiology chart

review was performed to determine the largest diameter of the tumor from the computed tomography scan before surgical resection. Patients were followed according to the standard of care, typically with biannual surveillance computed tomography imaging until censoring or death. Patients who chose to terminate surveillance imaging were censored at the last date of surveillance. Once patients were enrolled in the IRB study, tissue was stored in the Vanderbilt Thoracic Biorepository with standardized follow-up to update clinical information.

Tissue Microarray Development

A tissue microarray (TMA) was developed from 1-mm diameter biopsy core punches from resected tumor tissue. Only primary tumor tissue and only tissue collected from the first resection were used. All patients had two tumor tissue core punches added to the TMA each taken from regions of the tumor tissue separated at least 3 mm. Patient tissue was banked at the time of resection, and all tumor punches were collected and used to build the TMA at the time of this analysis. Patient selection was performed before any analysis of the immune microenvironment.

Multiplex Immunofluorescence Staining and Analysis

The TMA was analyzed using mxIHC, using the procedure described in detail previously.²⁷ The panel contained 4',6-diamidino-2-phenylindole (DAPI) (to identify cell nuclei), and staining for cytokeratins using Opal650 dye with antibody clone AE1/AE3 from Agilent DAKO (Agilent, Santa Clara, CA) (to identify tumor areas). The panel also contained five markers for immune cells: CD3 stained using Opal520 dye with antibody clone 2GV6 from Ventana Medical Systems (Oro Valley, Arizona) (to identify T-lymphocytes), CD20 stained using Opal540 dye with antibody clone L26 from Ventana Medical Systems (to identify B-lymphocytes), CD117 stained using Opal690 dye with antibody clone c-kit from Agilent DAKO (to identify mast cells), FOXP3 using Opal620 dye with antibody clone SP97 from Abcam (Waltham, MA) (to identify regulatory T-cells), and Ki67 using Opal570 dye with antibody clone 30-9 from Ventana Medical Systems (to identify proliferation within the other cell phenotypes). Emission spectra were unmixed and stained tissue core images were captured using Vectra spectral imaging system (Akoya Bioscience, Marlborough, MA). For cell segmentation, nuclear staining with DAPI was used to locate each cell using an automated algorithm that was previously validated.²⁷ Phenotyping was performed by annotating different types of cells on images with combinations of known

markers as described previously. For example, tumor cells were defined as any cell that was CK⁺, CD3⁻, CD20⁻, CD117⁻, whereas T-cells were defined as CD3⁺, CK⁻, CD20⁻, CD117⁻. Tissue was classified as either "tumor" or "stroma" according to the proximity of CK⁺ staining, and the area occupied by each tissue type was calculated on the basis of these classifications in mm². The total cell counts for each cell phenotype and the area occupied by each tissue type were used to calculate the density of cell populations in each tissue type in cells/mm².

Study Outcome

The RFS was counted from the date of surgical resection. The primary outcome of the study was RFS, so recurrence or death was considered equivalent. Recurrence status was ascertained from medical records after the TMA analysis had been performed. Patients were followed annually for up to 14 years, with a median follow-up of 6 years (interquartile range [IQR]: 1.7–8.7 years) for patients who were lost to follow-up. For statistical analyses, survival data were censored at 6 years from the date of surgical resection. Recurrence was confirmed by histopathologic diagnosis.

Statistical Analysis

An analysis of the variation of cell densities within the two punches from the same person was performed to evaluate bias, by calculating the variation in cell densities between duplicate punches from the same tumor using Spearman's correlation, and only analyzing cellular populations with highly correlated densities (lower 95% confidence interval [CI] of Spearman's r ρ > 0.5). For statistical analysis, each patient was counted once, to ensure even weighting. Patients with successfully stained duplicate cores had the analyzed metrics averaged. Patients with only a single successfully stained core used the values from the single core. Summary values were obtained for the median and IQR for all continuous variables, and as frequency and percentage of whole for binary and categorical variables. No missing values were observed for any of the study variables. The Kaplan-Meier (K-M) method was used to estimate the RFS of four groups on the basis of quartiles of immune response distribution for visualization. The quartile (Q) groups were the lowest 25% of values (the smallest value \leq group 1 $<$ Q 1), the next lowest 25% of values (Q 1 \leq group 2 $<$ median), the second highest 25% of values (median \leq group 3 $<$ Q 3) and the highest 25% of values (group 4 \geq Q3). In the RFS (K-M) plot, the hazard ratio (HR) of recurrence or death with 95% CI was reported per IQR change in a continuous predictor (e.g., an immune response) on the basis of a univariate Cox regression model. In addition, the adjusted (adj.) HR

was on the basis of a multivariable Cox regression model. A multivariable Cox regression model was performed for investigating the association between RFS and cell densities adjusted for sex and EGFR mutation status. The proportional-hazards assumption was evaluated using a chi-square goodness-of-fit test and graphical diagnostics on the basis of the scaled Schoenfeld residuals. For the relationship between T-cells and characteristics or between mast cells and the characteristic, the difference in cell density with a 95% CI between two groups for each characteristic was calculated on the basis of the Wilcoxon rank sum test. The strength and direction of association between cell density and each ordinal or continuous characteristic were measured using Spearman's rank correlation coefficient ρ with 95% CI. All statistical analysis was performed using R version 4.1.2 (R Core Team, Vienna, Austria).²⁸ Survival analysis was performed using packages "survival" and "survminer."²⁹ The two-sided 95% CI was used for all statistical tests. The analyses did not adjust for type I error to account for multiple types of immune cell testing.

Results

Patients' Characteristics and Their Association With LUAD Recurrence

A total of 100 patients with surgically resected stage I and II LUAD were included in this study, 30 with subsequent recurrence and 70 without. A CONSORT diagram of patient inclusion is presented in Figure 1. There were no substantial differences in ethnic makeup, age at diagnosis, smoking status at diagnosis, and nodule size on imaging. Mutation status testing of the tumor tissue was performed according to the standard of care, and the results revealed distributions of the most common mutations which are similar to those previously reported (KRAS mutation was present in 31% of patients, EGFR in 12%) (Table 1). Cancer stage, age of the patient at resection, body mass index (BMI), and smoking status were not significantly different between patients in the recurrence and no recurrence groups. There was no noteworthy association between smoking status and recurrence, BMI and recurrence, or age at collection and recurrence.

Multiplex Immunohistochemistry Revealed Different T-Cell and Mast Cell Densities Between Patients With and Without Recurrence

Figure 2 illustrates examples of the composite spectral fluorescence image (Fig. 2A). On the basis of the spectral intensities, each cell is automatically segmented and then assigned a phenotype (Fig. 2B). From the spatial distribution of cell phenotypes, the tissue is then

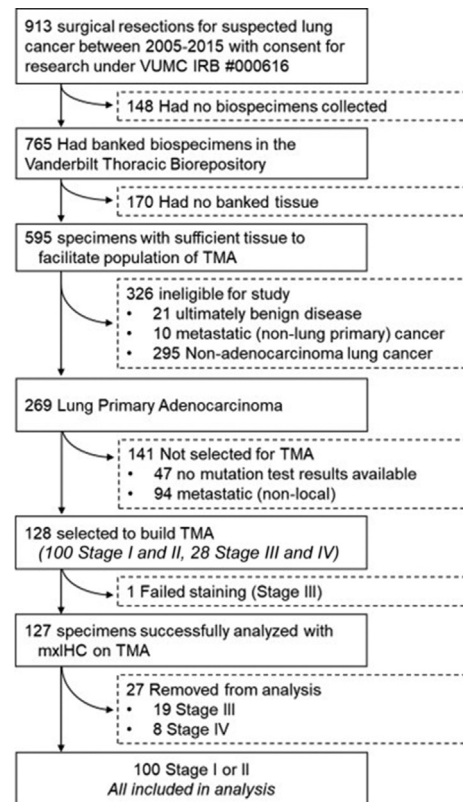


Figure 1. Consort Diagram of patient inclusion. mxIHC, multiplexed immunohistochemistry; TMA, tissue microarray; VUMC IRB, Vanderbilt University Medical Center Institutional Review Board.

automatically segmented into the tumor, stroma, and nontissue regions (Fig. 2C). We identified differences in survival associated with the density of several immune populations in the tumor compartment.

Recurrence-Free-Survival was Associated With Tumoral Immune Cell Densities

Patients were divided into four groups at the lower quartile (34.8 cells/mm²), the median (65.56 cells/mm²), and the upper quartile (112 cells/mm²) of tumoral T-Cell density. In the K-M plot, the RFS curves of four-level groups in tumoral T-cell presented a higher tumoral T-cell exhibited a higher RFS rate. For example, at 5 years, the RFS for each group of cell density is as follows: (1) group 1: 44% (CI: 26%–77%); (2) group 2: 48% (CI: 29%–81%); (3) group 3: 70% (CI: 53%–91%); (4) group 4: 84% (CI: 67%–0.99%), respectively. The HR in the KM plot was on the basis of the univariate Cox regression analysis. For every IQR increase in tumoral T-Cell density, the risk of disease recurrence or death will decrease by 49% on the basis of HR per IQR increase of 0.51 (CI: 0.27–0.97). That is, a high level of tumoral T-cell was associated with a favorable RFS rate. (Fig. 3A). There was not sufficient evidence to illustrate the

Table 1. Population Characteristics for Stage I and II, Split by Outcome (Recurrence Versus No Recurrence)

Variable	All		By Recurrence			
			No		Yes	
Age (y)	67	(60-71)	67	(61-72)	66	(59-70)
Sex						
Female	53	(53)	41	(59)	12	(40)
Male	47	(47)	29	(41)	18	(60)
Smoking status						
Current smoker	15	(15)	10	(14)	5	(17)
Former smoker	69	(69)	48	(69)	21	(70)
Never smoked	16	(16)	12	(17)	69	(13)
Ex or current smoker	84	(84)	58	(83)	26	(87)
Race						
African American	5	(50)	3	(4)	2	(7)
Asian	1	(10)	1	(1)	0	-
White	93	(93)	65	(93)	28	(93)
Unknown or other	1	(10)	1	(14)	0	-
Prior cancer	40	(40)	27	(39)	13	(43)
Path stage						
Stage I	69	(69)	51	(73)	18	(60)
Stage II	31	(31)	19	(27)	12	(40)
BMI	26	(23-30)	26	(23-30)	25	(23-28)
Any mutation	46	(47)	31	(45)	15	(50)
AKT1	0	—	0	—	0	—
BRAF	3	(3)	3	(4)	0	—
EGFR	12	(12)	8	(11)	4	(13)
PIK3CA	2	(2)	1	(1)	1	(3)
KRAS	31	(31)	21	(30)	10	(33)
Missing	1		1		0	
Chemo	24	(24)	10	(15)	14	(47)
Missing	1		1		0	
Radiation	7	(7)	4	(6)	3	(10)
Missing	1		1		0	
Tumor size (mm)	23	(17-32)	23	(17-30)	26	(17-38)
Tumoral cell densities (cells per square micron)						
B-cells (-)	0.9	(0.2-2.7)	0.9	(0.3-3.7)	0.9	(0.06-1.8)
B-cells (+)	0	(0-0.72)	0	(0-0.65)	0.8	(0-0.78)
Mast cells	2.8	(0.8-7.5)	4.2	(1.5-10)	1.5	(0.46-3.2)
T-cells (-)	66	(35-112)	74.2	(41-127)	46.8	(29-71)
T-cells (+)	3.9	(2.3-7.4)	4.0	(2.3-7.6)	3.6	(2.3-7.0)
T-regulators	0.3	(0-1)	0.3	(0-1.2)	0.3	(0-0.8)

Note: Continuous variables represented as: median (interquartile range). Categorical values represented as n (%).

BMI, body mass index; Chemo, chemotherapy.

association between RFS and the proliferating T-cells (Ki67+) (HR per IQR increase = 0.919, CI 0.59–1.42).

When the patient population was split into four groups on the basis of the lower quartile (0.84 cells/mm²), the median (2.8 cells/mm²), and the upper quartile (7.52 cells/mm²) of tumoral mast cells density, the K-M plot illustrated the patients in higher tumoral mast cell density (for comparing group 4 versus group 1) had better RFS rate. The risk of RFS was reduced by 65% for every IQR change in tumoral mast cell density (HR per IQR = 0.35, CI: 0.15–0.8) (Fig. 3B).

The immune cell densities were each adjusted for sex and EGFR mutation status, in a multivariable Cox

regression model, and this analysis revealed that even with adjustment, T-cell densities (adj. HR per IQR increase = 0.50, CI: 0.27–0.93) (Fig. 3A) and tumoral mast cell (adj. HR per IQR increase = 0.36, CI: 0.15–0.84) (Fig. 3B) were significantly associated with recurrence-free-survival (Supplementary Table 1).

High Tumoral T-Cells are Associated With a Higher Density of Other Immune Populations

We further investigated the relationship between tumoral T-cells density and other clinical characteristics and other immune populations or between mast cell density

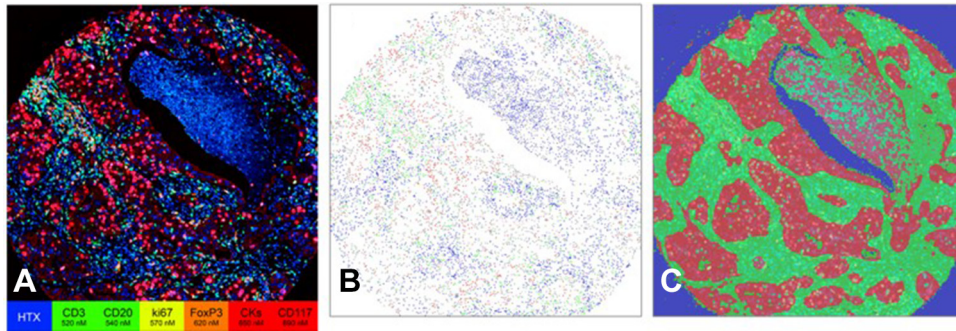


Figure 2. mxIHC staining of tumor punches allows spatially resolved cell identification. (A) Composite staining images are collected using the Vectra spectral imaging system. (B) Each cell’s phenotype was determined from the staining intensities so that a phenotype for each cell can be assigned to a specific location. Each dot represents one cell, and the color indicates the cell phenotype. (C) The distribution of cell types is used to segment tumor (red), stroma (green), and nontissue (blue) regions. HTX, hematoxylin; mxIHC, multiplexed immunohistochemistry.

and other clinical characteristics and other immune populations. The rank order of T-cell densities is correlated with the rank order of B-cell densities (Spearman’s rank correlation coefficient [Spearman’s ρ] = 0.54, CI: 0.38–0.66), proliferating T-cell densities (Spearman’s ρ = 0.37, CI: 0.19–0.53), and mast cell densities (Spearman’s ρ = 0.23, CI: 0.04–0.41). Mast cell density is positively correlated with B cells (Spearman’s ρ = 0.27, CI: 0.08–0.45), T-cells (Spearman’s ρ = 0.23, CI: 0.04–0.41), T-regulators (Spearman’s ρ = 0.24, CI: 0.05–0.42), but negatively correlated with cytokeratin (+) (Spearman’s ρ = –0.21, CI: –0.39 to –0.01) (Tables 2 and 3).

Discussion

LUAD exhibits a wide range of biological behaviors. Some adenocarcinomas may remain indolent for years,

whereas others behave more aggressively and require early detection and treatment. In fact, some adenocarcinomas will recur despite complete surgical resection, with or without adjuvant or neoadjuvant therapy, whereas other morphologically similar tumors may remain stable without treatment for prolonged periods.³⁰ The biological underpinning of this difference in aggressiveness is still poorly understood, although past studies have reported strong links between several molecular markers and aggressiveness.³¹ Most studies have focused on the biological characteristics of the tumor itself, but the ability of the immune response to contain tumor growth is an alternative area of investigation.

In this study, we sought to investigate the relationship between the TME and the likelihood of recurrence for early-stage LUAD. We used an mxIHC

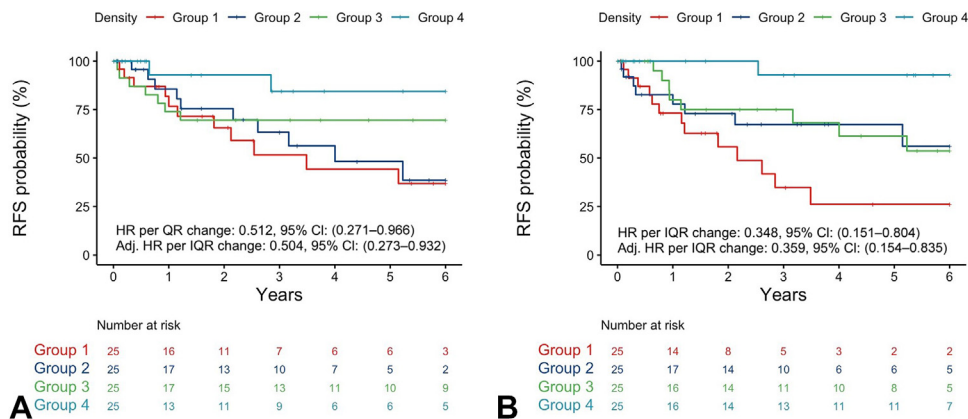


Figure 3. Kaplan-Meier survival curves of recurrence-free-survival of four groups on the basis of quartile of cell density distribution in the early stage. (A) Tumoral T-cell density—group 1: (3.24–34.8), group 2: (34.8–65.56), group 3: (65.56–112), group 4: (112–370.6) per mm² of tumor tissue. (B) Tumoral mast cell density—group 1: (0–0.84), group 2: (0.84–2.8), group 3: (2.8–7.52), group 4: (7.52–134.96) per mm² of tumor tissue. HR represented as HR per IQR increase in cell density on the basis of the univariate Cox model. Adj. HR stood for the adjusted hazard ratio on the basis of the multivariable Cox model adjusted for sex and EGFR mutation status. Adj., adjusted; CI, confidence interval; HR, hazard ratio; IQR, interquartile range; RFS, recurrence-free survival.

Table 2. Difference in Cell Density Between Each Characteristic (Two Groups)

Variables	Tumoral T Cells Density			Tumoral Mast Cells Density		
	Difference in Location (CI)		p-Value	Difference in Location (CI)		p-Value
Sex (female vs. male)	-2	(-7.235 to 2.835)	0.384	-0.02	(-0.35 to 0.33)	0.871
Ex or current smoker (no vs. yes)	0.965	(-6.07 to 8.245)	0.781	-0.01	(-0.51 to 0.433)	0.985
Race (other vs. White)	-4.39	(-14.525 to 5.46)	0.373	-0.01	(-0.89 to 0.81)	0.946
Prior cancer (no vs. yes)	3.861	(-1.12 to 9.42)	0.129	0.072	(-0.235 to 0.447)	0.602
Path stage (stage I vs. stage II)	4.905	(-0.09 to 10.505)	0.052	0.275	(-0.02 to 0.66)	0.07
Any mutation (no vs. yes)	-0.17	(-4.955 to 4.785)	0.934	0.12	(-0.165 to 0.555)	0.475
BRAF (no vs. yes)	-14.05	(-28.258 to 3.28)	0.086	-0.14	(-1.815 to 2.015)	0.708
EGFR (no vs. yes)	1.213	(-5.545 to 9.44)	0.707	0.105	(-0.29 to 0.735)	0.644
PIK3CA (no vs. yes)	-4.785	(-17.3 to 20.865)	0.514	-0.6	(-2.355 to 4.695)	0.369
KRAS (no vs. yes)	1.135	(-4.465 to 6.465)	0.704	0.1	(-0.195 to 0.52)	0.531
Chemo (no vs. yes)	2.507	(-3.25 to 8.27)	0.354	0.3	(-0.01 to 0.79)	0.064
Radiation (no vs. yes)	-9.268	(-16.485 to 0.49)	0.062	0.485	(0 to 1.465)	0.046

Note: Difference in location (CI): the difference in location of cells density between each variable group with 95% CI based on Wilcoxon rank sum test. No patient with AKT1 mutation.

Chemo, chemotherapy; CI, confidence interval.

(multiplex immunofluorescence) panel that was previously developed and optimized for TME profiling. The markers were selected on the basis of recommendations of the Molecular and Cellular Characterization of Screen-Detected Lesions (MCL: <https://mcl.nci.nih.gov/>) pathologists working group and looked at the densities of T-cells, mast cells, B cells, T-regulator cells, and cancer cells. This analysis revealed that the density of T-cells and mast cells was associated with RFS (Fig. 3). Interestingly, variables typically associated with clinical outcomes such as BMI, patient age, or smoking status were not found to be predictive of overall survival or RFS, although it is possible that our study was underpowered to detect these associations. The only clinical variable strongly associated with RFS was sex, with a proportional hazard of 2.66 for men (95% CI: 1.28–5.55). This is consistent with past reports on RFS,³² overall survival,³³ and immune infiltration,³⁴ which

have suggested that women with LUAD seem to fare better than men. To take into account the impact of confounding factors on the RFS, with the rule of at least 10 events per variable, sex, and EGFR mutation status were considered in multivariable analysis. Cox regression model adjusted for sex and EGFR mutation status also revealed similar results (adj. HR per IQR increase in tumoral T-cell density = 0.53, CI: 0.29–0.98; adj. HR per IQR increase in tumoral mast cell density = 0.37, CI: 0.15–0.87) (Supplementary Table 1) compared with the univariate Cox regression model (Supplementary Table 1). Interestingly, the first and second quartiles of T-cell density had similar RFS (44% and 48%, respectively), compared with the higher levels of the third and fourth quartiles (70% and 84%). The similarity in the first two quartiles suggests that perhaps there is a minimum biologically relevant level of T-cell infiltration before a protective effect is gained. Further

Table 3. The Rank Correlation Between Cell Density and Each Continuous Characteristic

Variables	Tumoral T Cells Density			Tumoral Mast Cells Density		
	Spearman's ρ (CI)		p-Value	Spearman's ρ (CI)		p-Value
Age (y)	0.14	(-0.058 to 0.328)	0.164	-0.001	(-0.197 to 0.196)	0.993
BMI	0.102	(-0.096 to 0.292)	0.313	0.062	(-0.136 to 0.255)	0.541
Tumor size	-0.075	(-0.268 to 0.124)	0.461	0.002	(-0.196 to 0.199)	0.988
Tumoral B-cells (-)	0.537	(0.381-0.663)	<0.001	0.274	(0.082-0.447)	0.006
Tumoral B-cells (+)	0.038	(-0.159 to 0.233)	0.704	0.07	(-0.128 to 0.263)	0.487
Tumoral cytokeratin (-)	-0.086	(-0.278 to 0.112)	0.394	0.087	(-0.112 to 0.278)	0.391
Tumoral cytokeratin (+)	0.096	(-0.102 to 0.287)	0.342	-0.207	(-0.388 to -0.011)	0.039
Tumoral mast cells	0.231	(0.036-0.409)	0.021			
Tumoral T-cells (-)				0.231	(0.036-0.409)	0.021
Tumoral T-cells (+)	0.372	(0.189-0.53)	<0.001	0.072	(-0.126 to 0.264)	0.478
Tumoral T-regulators	0.29	(0.099-0.46)	0.003	0.24	(0.046-0.417)	0.016

Note: Spearman's rho (CI): Spearman's rank correlation coefficient between cells density and each variable with 95% CI.

BMI, body mass index; CI, confidence interval.

studies in larger cohorts are required to more thoroughly address this.

The staining panel used here included markers for T-cells (CD3), regulatory T cells (FOXP3), B cells (CD20), mast cells (CD117), tumor cells (CK), and a proliferation marker (Ki67), in addition to DAPI. These markers were chosen to enable visualization of the interplay between these immune populations and the tumor/stromal tissue. Several combinations of markers and antibodies were explored to optimize this panel, which has been detailed in previous work.²⁷ Particularly, mast cells were chosen because of the conflicting reports of their prognostic indication in previous studies; further study of their role in lung primary cancer is warranted. Several other immune-phenotype panels have been developed, or are in development, which focuses on other immune cell populations, such as natural killer cells and monocytes, which will be included in future work.

There is a critical need to identify clinical biomarkers to predict recurrence after surgical treatment of LUAD to inform patient care, as current management of LUAD is on the basis of tumor stage, mutation status, and in some cases programmed death-ligand 1 (PD-L1) expression status. Aggressiveness has been predicted using radio mic-based tools³⁵ and comprehensive histologic evaluation,^{36–38} but these rely primarily on tumor-specific characteristics and ignore the potential impact of patient-specific immune response to the tumor.³⁹ An improved method to gauge aggressiveness and predict recurrence would provide physicians with a tool to help guide individualized adjuvant treatment and a follow-up approach specifically tailored to each patient. Being able to characterize the TME as an independent predictor of recurrence after surgical treatment may have important clinical implications: whereas tumor biological predictors may be associated with short-term recurrence, the inability to mount an adequate local immune response, which is a function of the host ability to constrain tumor progression, may have implications on the longer-term risk of developing new malignancies, thus requiring longer surveillance.

There was a large difference in the number of patients who underwent chemotherapy in the recurrence and recurrence-free groups. The decision to treat with chemotherapy was made by the care team in communication with the patient, following the National Comprehensive Cancer Center guidelines, and did not use the results of this staining panel. However, the standard of care uses PD-L1 staining in the decision to use some chemotherapies, and for this reason, the densities of PD-L1 and their relation to the immune populations studied here are a focus of ongoing work by our group, and the relation between CD8 versus CD4 T-cells, other immune populations, and patient outcomes.

There are several limitations to this study. First is an inherent limitation of real-world analysis of the RFS, which cannot, by definition, exclude subclinical recurrence at the time of death or loss to follow-up. Therefore, some patients who did not have a clinical recurrence may have expressed markers indicative of recurrence. However, a subclinical recurrence is arguably less clinically important than a clinically obvious one. Another limitation is the limited sample size, the fact that the type I error was not adjusted for multiple testing, and the lack of an independent validation set. Therefore, these results await validation in additional studies. An additional limitation is the automated cell segmentation and classification method, used in this study, which has a small rate of misclassification; however, this panel and segmentation method was previously tested and extensively validated.²⁷ Therefore, this does not likely introduce bias. Within the patients included in our study, BMI, smoking history, and known genetic mutations (EGFR, KRAS, BRAF, PIK3CA, and AKT1) were not associated with the likelihood of recurrence, although past studies have reported a relationship between these predictors and outcomes. For example, EGFR mutation has been linked to increased rates of metastatic recurrence in patients with early-stage LUAD who had a recurrence (i.e., the rate of distant recurrence), but not linked to the overall rate of recurrence when considering local and metastatic cancers.⁴⁰ The lack of association for these predictors in the patients presented here is likely a type II error because of the sample size. Another major limitation is the lack of markers in this study for the identification of innate immune cells (macrophages, neutrophils, dendritic cells, and natural killer cells), which are known to have an important role in tumor progression.⁴¹ Finally, there was a long accrual time for patients in this study. During the accrual period (2005–2015), the approach to lung cancer TNM staging was updated from the sixth edition (2002–2009) to the seventh edition (2010–2016). However, the updates to staging did not affect who would have been included in this study, as the largest change in early-stage classification was the division of stage I into stages Ia and Ib, and stage II into stages IIa and IIb.⁴² Only nine of the patients included in the study had their primary surgery before 2010 when this change went into effect (Supplementary Fig. 1). Similarly, during this same period, the National Comprehensive Cancer Network's recommendation for early-stage LUAD did not change.

In conclusion, an mxIHC panel to visualize spatial distributions of immune cells within surgically resected LUADs revealed that there is an association between the density of immune infiltration and the likelihood of recurrence. These results suggest that the

range of aggressiveness within adenocarcinomas may be a result of the immune system interactions with the tumor, not only the makeup of the tumor itself. Immune TME characterization could represent a novel biomarker to facilitate tailored management of adenocarcinoma and a guide to follow-up after treatment.

Credit Author Statement

Michael N Kammer: Investigation, Writing – original draft, Visualization.

Hidetoshi Mori: Investigation, Formal analysis, Methodology, Software.

Dianna J. Rowe: Data curation, Investigation.

Sheau-Chiann Chen: Formal analysis, Visualization, Writing – review & editing.

Georgii Vasiukov: Formal analysis, Methodology, Investigation.

Thomas Atwater: Conceptualization.

Maria Fernanda Senosain: Investigation.

Sanja Antic: Resources.

Yong Zou: Resources, Investigation.

Heidi Chen: Formal Analysis, Supervision.

Tobias Peikert: Writing – review & editing.

Steve Deppen: Writing – review & editing.

Eric Grogan: Writing – review & editing, Supervision.

Pierre P. Massion: Writing – review & editing, Conceptualization, Investigation, Methodology, Resources, Funding acquisition.

Steve Dubinett: Writing – review & editing, Methodology, Resources, Funding acquisition.

Marc Lenburg: Writing – Review & Editing, Methodology, Resources, Funding acquisition.

Alexander Borowsky: Writing – review & editing, Methodology, Resources, Funding acquisition.

Fabien Maldonado: Writing – review & editing, Supervision.

Acknowledgments

This work was supported by the National Cancer Institute (NCI)/National Institutes of Health (NIH) (CA196405 to Dr. Massion and U01CA196406 to Dr. Borowsky). The funding source did not have access to the data, results, or manuscript before publication. This work is a result of the vision of our dear mentor and friend, Dr. Pierre P. Massion.

Supplementary Data

Note: To access the supplementary material accompanying this article, visit the online version of the *JTO Clinical and Research Reports* at www.jtocrr.org and at <https://doi.org/10.1016/j.jtocrr.2023.100504>.

References

1. Miller KD, Fidler-Benaoudia M, Keegan TH, Hipp HS, Jemal A, Siegel RL. Cancer statistics for adolescents and young adults, 2020. *CA Cancer J Clin.* 2020;70:443-459.
2. Siegel RL, Miller KD, Jemal A. Cancer statistics, 2020. *CA Cancer J Clin.* 2020;70:7-30.
3. Patz EF Jr, Pinsky P, Gatsonis C, et al. Overdiagnosis in low-dose computed tomography screening for lung cancer. *JAMA Intern Med.* 2014;174:269-274.
4. Zhang J, Fujimoto J, Zhang J, et al. Intratumor heterogeneity in localized lung adenocarcinomas delineated by multiregion sequencing. *Science.* 2014;346:256-259.
5. de Bruin EC, McGranahan N, Mitter R, et al. Spatial and temporal diversity in genomic instability processes defines lung cancer evolution. *Science.* 2014;346:251-256.
6. Qian J, Zhao S, Zou Y, et al. Genomic underpinnings of tumor behavior in in situ and early lung adenocarcinoma. *Am J Respir Crit Care Med.* 2020;201:697-706.
7. Suzuki K, Kachala SS, Kadota K, et al. Prognostic immune markers in non-small cell lung cancer. *Clin Cancer Res.* 2011;17:5247-5256.
8. Coussens LM, Werb Z. Inflammation and cancer. *Nature.* 2002;420:860-867.
9. Brambilla E, Le Teuff G, Marguet S, et al. Prognostic effect of tumor lymphocytic infiltration in resectable non-small-cell lung cancer. *J Clin Oncol.* 2016;34:1223-1230.
10. Zeng DQ, Yu YF, Ou QY, et al. Prognostic and predictive value of tumor-infiltrating lymphocytes for clinical therapeutic research in patients with non-small cell lung cancer. *Oncotarget.* 2016;7:13765-13781.
11. Al-Shibli K, Al-Saad S, Andersen S, Donnem TOM, Bremnes RM, Busund L-T. The prognostic value of intra-epithelial and stromal CD3-, CD117- and CD138-positive cells in non-small cell lung carcinoma. *APMIS.* 2010;118:371-382.
12. Djenidi F, Adam J, Goubar A, et al. CD8+/CD103+ tumor-infiltrating lymphocytes are tumor-specific tissue-resident memory T cells and a prognostic factor for survival in lung cancer patients. *J Immunol.* 2015;194:3475.
13. Kayser G, Schulte-Uentrop L, Siene W, et al. Stromal CD4/CD25 positive T-cells are a strong and independent prognostic factor in non-small cell lung cancer patients, especially with adenocarcinomas. *Lung Cancer.* 2012;76:445-451.
14. Petersen RP, Campa MJ, Sperlazza J, et al. Tumor infiltrating Foxp3+ regulatory T-cells are associated with recurrence in pathologic stage I NSCLC patients. *Cancer.* 2006;107:2866-2872.
15. Schalper KA, Brown J, Carvajal-Hausdorf D, et al. Objective measurement and clinical significance of TILs in non-small cell lung cancer. *J Natl Cancer Inst.* 2015;107:dju435.
16. Tian C, Lu S, Fan Q, et al. Prognostic significance of tumor-infiltrating CD8+ or CD3+ T lymphocytes and interleukin-2 expression in radically resected non-small cell lung cancer. *Chin Med J (Engl).* 2015;128:105-110.
17. Al-Shibli KI, Donnem T, Al-Saad S, Persson M, Bremnes RM, Busund L-T. Prognostic effect of epithelial

- and stromal lymphocyte infiltration in non-small cell lung cancer. *Clin Cancer Res.* 2008;14:5220.
18. Wakabayashi O, Yamazaki K, Oizumi S, et al. CD4+ T cells in cancer stroma, not CD8+ T cells in cancer cell nests, are associated with favorable prognosis in human non-small cell lung cancers. *Cancer Sci.* 2003;94:1003-1009.
 19. Donnem T, Hald SM, Paulsen E-E, et al. Stromal CD8+ T-cell density—a promising supplement to TNM staging in non-small cell lung cancer. *Clin Cancer Res.* 2015;21:2635.
 20. Ilie M, Hofman V, Ortholan C, et al. Predictive clinical outcome of the intratumoral CD66b-positive neutrophil-to-CD8-positive T-cell ratio in patients with resectable nonsmall cell lung cancer. *Cancer.* 2012;118:1726-1737.
 21. Kawai O, Ishii G, Kubota K, et al. Predominant infiltration of macrophages and CD8+ T cells in cancer nests is a significant predictor of survival in stage IV nonsmall cell lung cancer. *Cancer.* 2008;113:1387-1395.
 22. Ruffini E, Asioli S, Filosso PL, et al. Clinical significance of tumor-infiltrating lymphocytes in lung neoplasms. *Ann Thorac Surg.* 2009;87:365-372.
 23. Suzuki K, Kadota K, Sima CS, et al. Clinical impact of immune microenvironment in stage I lung adenocarcinoma: tumor interleukin-12 receptor $\beta 2$ (IL-12R $\beta 2$), IL-7R, and stromal FoxP3/CD3 ratio are independent predictors of recurrence. *J Clin Oncol.* 2013;31:490-498.
 24. Senosain MF, Zou Y, Novitskaya T, et al. HLA-DR cancer cells expression correlates with T cell infiltration and is enriched in lung adenocarcinoma with indolent behavior. *Sci Rep.* 2021;11:14424.
 25. Neophytou CM, Pierides C, Christodoulou M-I, Costeas P, Kyriakou T-C, Papageorgis P. The role of tumor-associated myeloid cells in modulating cancer therapy. *Front Oncol.* 2020;10:899.
 26. Bao X, Shi R, Zhao T, Wang Y. Mast cell-based molecular subtypes and signature associated with clinical outcome in early-stage lung adenocarcinoma. *Mol Oncol.* 2020;14:917-932.
 27. Mori H, Bolen J, Schuetter L, et al. Characterizing the tumor immune microenvironment with tyramide-based multiplex immunofluorescence. *J Mammary Gland Biol Neoplasia.* 2020;25:417-432.
 28. R Core Team. Pages. Accessed at R Foundation for Statistical Computing. Accessed October 15, 2022. <https://www.R-project.org/>
 29. Therneau TM, Grambsch PM. *Modeling Survival Data: Extending the Cox Model.* New York, NY: Springer; 2000.
 30. Thalanayar PM, Altintas N, Weissfeld JL, Fuhrman CR, Wilson DO. Indolent, potentially inconsequential lung cancers in the Pittsburgh lung screening study. *Ann Am Thorac Soc.* 2015;12:1193-1196.
 31. Guan H, Zhu T, Wu S, et al. Long noncoding RNA LINC00673-v4 promotes aggressiveness of lung adenocarcinoma via activating WNT/ β -catenin signaling. *Proc Natl Acad Sci U S A.* 2019;116:14019-14028.
 32. Watanabe K, Sakamaki K, Nishii T, et al. Gender differences in the recurrence timing of patients undergoing resection for non-small cell lung cancer. *Asian Pac J Cancer Prev.* 2018;19:719-724.
 33. Sakurai H, Asamura H, Goya T, et al. Survival differences by gender for resected non-small cell lung cancer: A retrospective analysis of 12,509 cases in a Japanese lung cancer registry study. *J Thorac Oncol.* 2010;5:1594-1601.
 34. Behrens C, Rocha P, Parra ER, et al. Female gender predicts augmented immune infiltration in lung adenocarcinoma. *Clin Lung Cancer.* 2021;22:e415-e424.
 35. Clay R, Rajagopalan S, Karwoski R, Maldonado F, Peikert T, Bartholmai B. Computer Aided Nodule Analysis and Risk Yield (CANARY) characterization of adenocarcinoma: radiologic biopsy, risk stratification and future directions. *Transl Lung Cancer Res.* 2018;7:313-326.
 36. Boland JM, Froemming AT, Wampfler JA, et al. Adenocarcinoma in situ, minimally invasive adenocarcinoma, and invasive pulmonary adenocarcinoma—analysis of interobserver agreement, survival, radiographic characteristics, and gross pathology in 296 nodules. *Hum Pathol.* 2016;51:41-50.
 37. Yoshizawa A, Motoi N, Riely GJ, et al. Impact of proposed IASLC/ATS/ERS classification of lung adenocarcinoma: prognostic subgroups and implications for further revision of staging based on analysis of 514 stage I cases. *Mod Pathol.* 2011;24:653-664.
 38. Warth A, Muley T, Meister M, et al. The novel histologic International Association for the Study of Lung Cancer/American Thoracic Society/European Respiratory Society classification system of lung adenocarcinoma is a stage-independent predictor of survival. *J Clin Oncol.* 2012;30:1438-1446.
 39. Clay R, Kipp BR, Jenkins S, et al. Computer-Aided Nodule Assessment and Risk Yield (CANARY) may facilitate non-invasive prediction of EGFR mutation status in lung adenocarcinomas. *Sci Rep.* 2017;7:17620.
 40. Galvez C, Jacob S, Finkelman BS, et al. The role of EGFR mutations in predicting recurrence in early and locally advanced lung adenocarcinoma following definitive therapy. *Oncotarget.* 2020;11:1953-1960.
 41. Liu Q, Sun Z, Chen L. Memory T cells: strategies for optimizing tumor immunotherapy. *Protein Cell.* 2020;11:549-564.
 42. Goldstraw P. The 7th edition of the TNM Classification for Lung Cancer: Proposals from the IASLC Staging Project. *Eur J Cancer Suppl.* 2007;5:15-22.